A Real-time EMF Measuring System for Mobile Communication Towers in Sri Lanka

Lakshitha Rangana WICKRAMASINGHE[1], Sisaara PERERA[2]

(1. *Sri Lanka Telecom*, *PLC*, *Lotus Road*, *Colombo*, *Sri Lanka;*
2. *The Open University of Sri Lanka*, *Nawala*, *Nugegoda*, 10250, *Sri Lanka.*)

Abstract: Telecommunications Regulatory Commission of Sri Lanka is the governing body which is responsible for the frequency allocation and monitoring the unauthorized Electromagnetic frequency (EMF) signal transmitting violations. However, in Sri Lanka, currently there is not any proper mechanism to monitor the radiation hazard level and its impact to the people living in the vicinity of mobile communication towers. There are approximately 7000 mobile transmitting towers in Sri Lanka to date and the used frequency range lies between 900MHz to 3GHz for mobile communication. Over the last few decades, many of the health hazard conditions were reported due to the radiation of those harmful EMFs. To cater this problem, a portable real time EMF signal strength measuring system with a radiation hazard level indicator was developed to monitor the EMF level and its impact. The proposed system operates with three intermediate frequency bands (i.e.900MHz, 1800MHz and 2400MHz) and it's capable of measuring the power density and the radiation hazard level at that particular point which is being measured. Moreover, the corresponding radiation hazard level is indicated with reference to the standard power density levels published by the International Commission on Non-Ionizing Radiation Protection (ICNIRP*). The system works with the overall accuracy of 88% in terms of identifying the power densities and its corresponding radiation hazard levels.

Keywords: Electromagnetic Frequency (EMF), Mobile Communication, Power Density, Radiation Hazard

1 Introduction

Electromagnetic spectrum can be introduced as the range of frequencies produced by all sources of electromagnetic radiation. Even though, all electromagnetic waves travel at the speed of light in a vacuum, it behaves in an identical way in a wide range of frequencies, wavelengths, and also in photon energies. The electromagnetic spectrum comprises with the span of all electromagnetic radiation and also contains many sub-ranges as mentioned in [1]. The major two energy types in the electromagnetic spectrum can be classified under the ionizing energy and non-ionizing energy.

Nowadays, there are many drawbacks and emerging health hazards can be found due to the exposure to harmful electromagnetic frequencies (EMFs)[2]. The main purpose of this research study is to identify those harmful electromagnetic levels and to notify the people in the vicinity of communication towers, regarding the impact of harmful radiation hazard levels. As mentioned earlier, health hazards due to harmful EMF radiation is at a critical stage. It has been found that the direct exposure to these harmful EMFs will reduce the life expectancy rate, can result in DNA damage, brain cell damage, aggressive growth in Leukemia cells and cancer cells, increased blood pressure rates, production of less sperm cells[2] etc. However, the possible causes for electromagnetic hazards are yet to be identified and as a solution, many research studies have been carried out over the past decades. In order to cater for this issue, many developed countries have taken policy decisions to control the growth of rapid and unnecessary telecommunication infrastructure facilities. However, this preliminary study was done related to the Sri Lankan context and we have proposed a novel real time approach to address the aforesaid issue.

At present there are 7000 telecommunication towers and approximately 33463471 mobile subscribers in Sri Lanka. The Telecommunications Regulatory Commission (TRC) of Sri Lanka [13] is the governing body which is responsible in providing regulations for the telecommunication infrastructure providers. However, Sri Lanka has adopted radiation norms and guidelines presented by *International Commission on Non-Ionizing Radiation Protection* (ICNIRP*) [3] for ensuring safe and prescribed measures. On the other hand, the ICNIRP guidelines clearly state that, for simultaneous exposure to multiple frequency fields, the sum of all the radiation strengths must be taken into consideration[3].

However, considering the Sir Lankan context, our study is primarily focused on investigating and identifying such higher radiation levels and addressing this radiation hazard issues.

Usually a smart mobile device (mobile phone) shows full strength of its signal levels at −69dBm input power and works satisfactorily in the received power range of −80 to −100dBm. In comparison with −80dBm level, the measured power level at 50m distance is at least 50 to 60 dB higher, which translates much higher and stronger signal than a mobile phone requires, in some circumstances. Moreover, depending upon the total number of transmitters in a particular area, there could be a probability that the people living near to those towers are to be exposed to radiation.

To cater these aforesaid issues, we have proposed and developed an internet of things(IoT) based electromagnetic field strength measuring system with an inclusive radiation hazard level detector.

The rest of the paper is organized as follows. In section 2, theoretical analysis introduces the currently available EMF measuring systems in Sri Lanka. In Section 3 we present the design methodology of the proposed electromagnetic field strength measuring system. Section 4 is dedicated for the measurements and operation of the prototype implementation. Finally, the Section 5 concludes the paper highlighting the future work of the proposed system.

2 Theoretical Analysis

2.1 Present Available Systems in TRC, Sri Lanka Tri-field EMF Meter

The tri-field EMF meter [4]is the widely used equipment at Telecommunications Regulatory Commission (TRC), Sri Lanka. This meter measures the radiation strengths of the antenna elements in vicinity fields. In addition, *Narda NBM 550* broad band field meter [5]is used alongside in order to obtain the relative EMF measurements. On the other hand, spectrum analyzers play a major role in measuring EMF data. TRC uses hand held spectrum analyzers for this purpose. Though there are variety of models, *Anritsu MS 2720T* 9kHz to[6] 43GHz analyzer is the commonly used analyzer for this purpose, as it is capable of measuring the variety of field strength and power measurements.

2.2 Automated Systems

In addition to the aforementioned field measuring system, TRC of Sri Lanka uses software defined vehicle based patrol system [7] for detection of strong EMF fields. It has seven antenna arrays in a dome fixed at the top of the vehicle by means of an antenna switching element. This antenna array can extend up to 10m in vertical direction. This operates through a software based system and also it can detect the range of frequencies starting from 3kHz to 6GHz. This is typically used for all island operations and which is also exorbitant in demand.

2.3 Theoretical Received Power by an Antenna

The power at the receiving antenna P_r at a distance R can be calculated by the following Friis Transmission formula [8].

$$P_r = P_t G_t G_r \left(\frac{\lambda}{4\pi R}\right)^2 \quad (1)$$

Where,

P_t = Output power of the transmitting antenna (W)

G_t= Gain of transmitting antenna

G_r = Gain of receiving antenna

R = Distance between the antennas (m)

λ= wave length of the signal

Friis formula indicates a measure of the received power, which is directly proportional to the transmitted power, gains of transmitting and receiving antennas, square of wavelength of the signal and it is inversely proportional to square of distance between the antennas.

2.4 Antenna Effective Aperture

Antenna aperture, effective area, or receiving cross section, is a measure of how effective an antenna operates at receiving the power of electromagnetic radiation. The aperture is defined as the area, oriented perpendicular to the direction of an incoming electromagnetic wave, which would intercept the same amount of power from that wave as is produced by the antenna receiving it.

The effective aperture of a duck type antenna is given by the following equation [9].

$$A_e = \frac{3\lambda^2}{8\pi} G \quad (2)$$

Where,

A_e= Effective aperture of antenna

λ= Wave length

G= Gain of the antenna

2.5 Conversion of Received Power to Power Density

Power density of a given antenna element can be calculated by dividing received power from effective aperture of the receiving antenna. Equation 3 shows the standard formula for calculating the power density.

$$S = \frac{8P\pi f^2}{3C_0^2 G_i} \quad (3)$$

Where,

P–Measured Power in Watts

G_i–Gain of receiving antenna in linear scale

f –Frequency of the EM wave

C_0–Velocity of light

Here the above equation is used to calculate the power density of each antenna element.

3 Design Methodology

The system block diagram of the proposed electromagnetic field measuring system is depicted in Fig.1.

In this system, three rubber duck antennas are used for the reception of 900 MHz, 1800 MHz and 2.4 GHz frequencies. Furthermore, the antenna elements are separately connected to EMF detectors through filter units. These EMF detectors convert the receiving power at particular instant to its corresponding DC values. The main controller used here is an ATMEGA 328P microcontroller and it converts analog EMF data to its corresponding digital values at the output. The respective power density level at the measuring point and its hazard level are displayed according to standard norms [3] and meantime the displayed data in that instant will be sent to an IoT server for the purpose of remote monitoring via a Node MCU. Moreover, the power requirement of the system is achieved by means of a rechargeable battery system which is powered by solar panels.

3.1 Antenna arrangement

In this project we have used separate special rubber duck antennas for better reception of EMF under 900MHz, 1800MHz and 2400MHz frequencies.

The rubber duck antenna can be considered as an electrically short monopole antenna which functions similar to a base-loaded whip antenna. In addition, it consists of a springy wire in the shape of a narrow helix, sealed in a rubber or plastic jacket to protect the antenna. Moreover, rubber duck antenna can be formed by means of a normal-mode helical antenna. On the other hand, it is also quite flexible than rigid telescopic antennas, which are specially designed for suitable

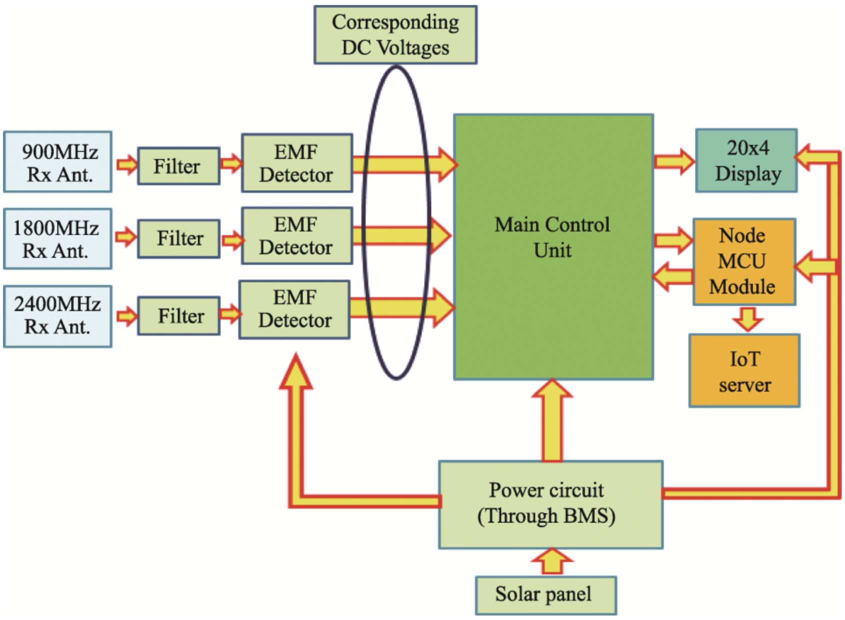

Fig.1 System Block Diagram

handheld operations, like wearing on a belt and on helmets etc. Furthermore, the length of this antenna is significantly smaller than the size of the effective aperture [9]. Therefore, the reception of EMF is slightly high in these types of antennas.

Besides, the rubber duck type antennas have somewhat better performance than an equal length based loaded antenna. Following Fig.2 depicted the duck type antenna elements for the aforesaid frequencies.

Fig.2 900MHz, 1800MHz, 2400MHz Ruber Duck Antennas

3.2 Band Pass Filter Units

Band pass filters can be used to isolate or filter out certain frequencies that lie within a particular band or range of frequencies. Here we have used separate, passive (LC) band pass filter unites for 900MHZ, 1800MHz and 2.4GHz frequencies respectively. The below section describes the design synthesis of the abovementioned band pass filter units.

Here the 5th order Butterworth band pass filter approximation is used to design the filter units [10]. The band pass filter topology at each frequency of operation is obtained by means of the two port network topology. The generalized frequency response of the 'n'th order Butterworth low pass filter approximation is given by the following equation.

$$H_{(j\omega)} = \frac{H_o}{\sqrt{1+\varepsilon^2\left(\frac{\omega}{\omega_p}\right)^{2n}}} \tag{4}$$

Where:

n −Order of the filter

ε −Maximum pass band gain (A_{max})

ω −Angular frequency

H_o −DC Gain

$H_{(j\omega)}$ −Frequency response transfer function.

Moreover, the filter design is realized in its normalized form in the two port network and the component scaling was done according to the following formulas.

$$C = \frac{C_n}{2\pi f_c R} \quad (5)$$

$$L = \frac{RL_n}{2\pi f_c} \quad (6)$$

Where:

C–Real capacitor value

L–Real inductor value

C_n–Normalized capacitor value

L_n–Normalized inductor value

R–Required load resistor value

f_c–Required 3dB-cut-off frequency

The designed filter units for 900MHZ, 1800MHz and 2.4GHz frequencies are shown in Fig.3, 4 and 5 respectively.

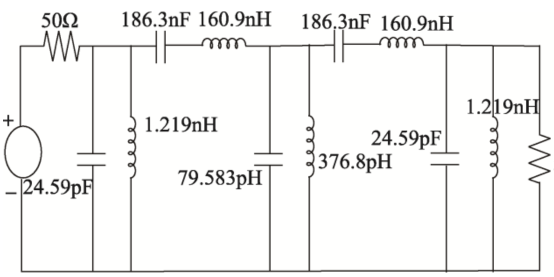

Fig.3 900MHz Band Pass Filter

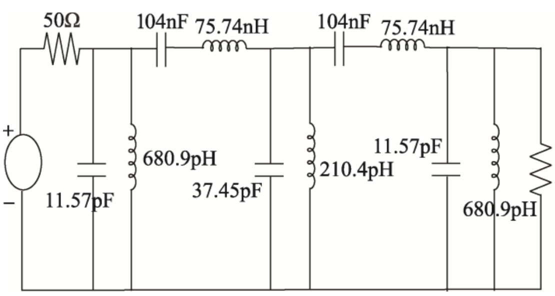

Fig.4 1800MHz Band Pass Filter

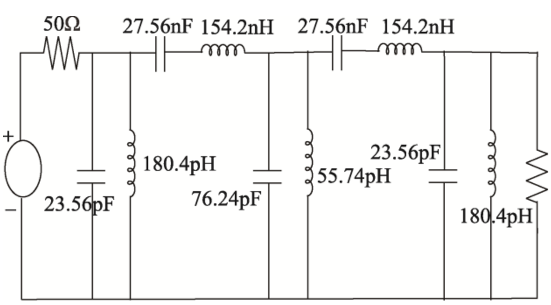

Fig.5 2400MHz Band Pass Filter

The 3dB lower and the upper cut-off levels of the band pass filter elements are shown in the following table 1.

Table 1 3dB Cut-off Levels of the Filter Units

Filter Frequency (MHz)	3dBLower Cut-off (MHz)	3dBUpper Cut-off (MHz)
900	880	960
1800	1170	1880
2400	2400	2484

3.3 IoT Module and the Control Unit

The concept of IoT can be described as a network of mutually connected physical devices embedded with software, sensors and actuators, which can be used for collecting and exchanging data. In simple, it is a standalone device which can be connected to a network and capable of running applications and interacting with the physical world. Here we have used Node MCU as the IoT module, which is a firmware based Wi-Fi module. It allows source free programming facility for the Wi-Fi module with a convenient form. Moreover, in the design synthesis, the AD8317 is a demodulating logarithmic amplifier and ATmega328P type microcontroller is used as the EMF detecting sensor and the main control unit, respectively.

3.4 Power Supply Unit

The proposed system is comprised of various equipment like, Microcontroller, Liquid crystal display (LCD) and a Node MCU unit etc. where the sub modules have different power requirements. To cater this, rechargeable Li-ion battery power management system (BMS) [11-12] is used alongside a regulated power supply. Furthermore, a 10W solar panel is used in the design model to provide an uninterrupted power to the battery system and further it is achieved through a LM2596 DC-DC buck converter. The overall block diagram of the power supply unit is illustrated in the following Fig.6

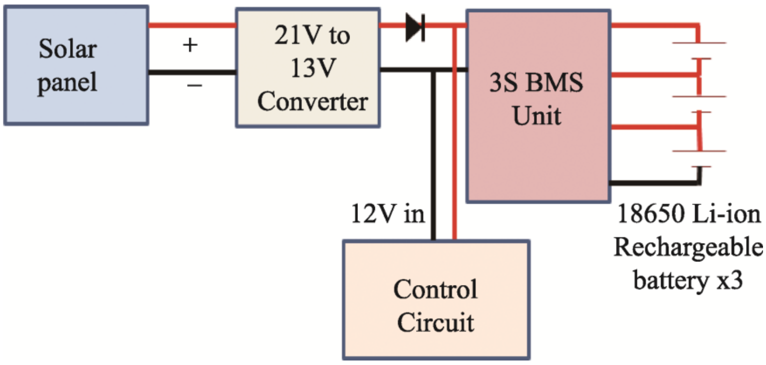

Fig.6 Block Diagram of Power Circuit

4 Measurements and Discussion

4.1 Operation and the Prototype Implementation

In order to calibrate sensor elements, the standard Anritsu MS 2720T spectrum analyzer[6] was used and the calibration results are tabulated in annexure 2. The complete proposed prototype of the system is illustrated in the Fig.7.

In the system prototype, 3 frequency selecting push buttons are used for the respective frequency of operation and the digital output and the radiation hazard level of the environment will be displayed according to the standard power density values in ICNIRP regulation, which is determined by the $f/200$, where f is the frequency in MHz [3].

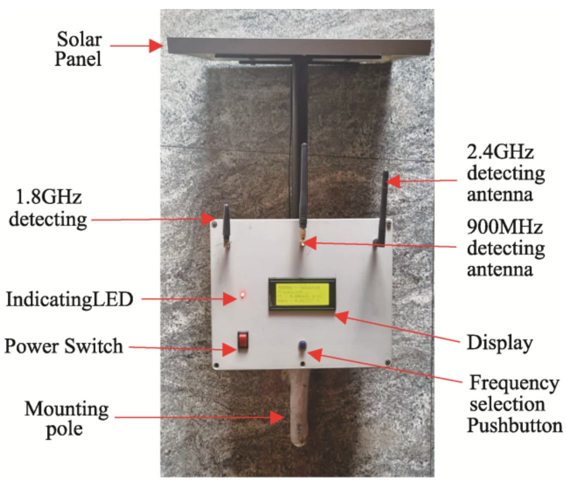

Fig.7 Proposed EMF Strength Measuring System

4.2 Test Results

The test results were obtained in near and far field of six mobile communication transmitting towers in Galle district, Sri Lanka during the month of January 2021. Moreover, the remotely obtained results of a pilot tower (tower 1-refer annexure 1) are illustrated in following Fig.8. The rest of the results are tabulated in annexure 1.

5 Conclusions

Sri Lanka is a country which has over 7000 telecommunication cell towers island wide. However, it has been reported that the harmful EMFs in mobile communication between 1800MHz and 3GHz has affected to people's lives over the past years, yet a proper study has not been conducted to measure and justify its impact. So, the proposed portable prototype of the EMF strength measuring module will provide an insight to the public about the hazard level in their living environment. This research was preliminary carried out in the Galle district, Sri Lanka and the results shows that the impact of radiation hazard is minimal in the district of Galle. Nowadays, IoT has become a crucial platform, which provides an easier approach to bring loads of information to one's fingertips. If the technical personnel can access the EMF data of a particular communication tower, measured via the proposed IoT system from anywhere, which would be a huge advantage for minimizing these hazards. Therefore, it directly helps to increase the total productivity and also to ensure the safe living

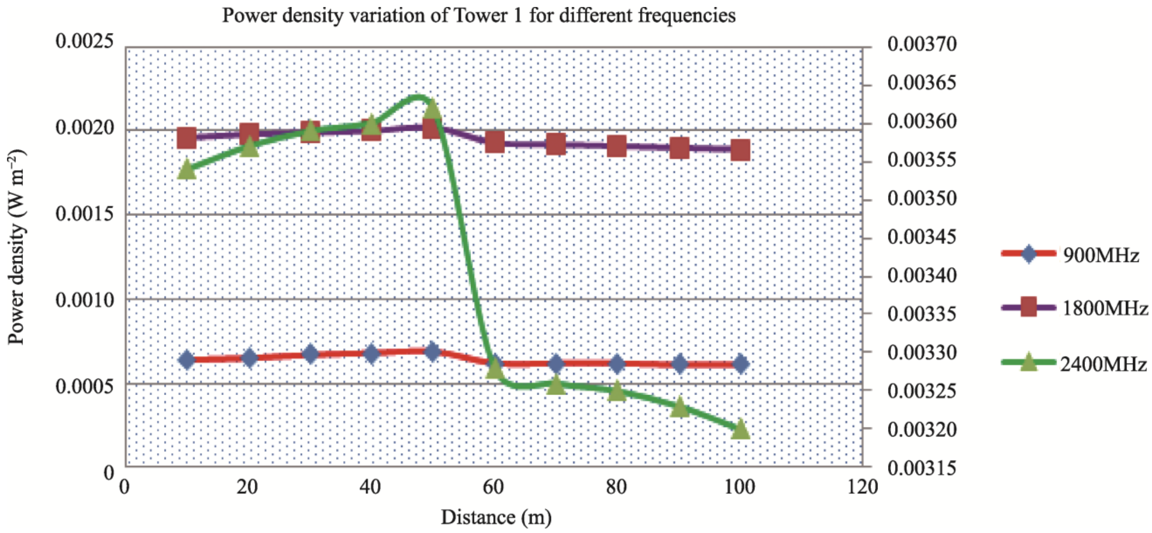

Fig.8 Power Density Variation of the Mobile Tower 1 for Different Frequencies

conditions of the people living in the vicinity of such towers. Furthermore, this is introduced as an IoT product of low cost, long life and with minimum maintenance. The contribution of this research can further be extended for island wide operation with facilitating proper infrastructure as this caters for remote monitoring of communication towers even in unreachable geographical conditions. However, design and implementation of hardware to withstand extreme environmental conditions was beyond the scope of this work, hence we categorize the same under future work.

Acknowledgement

The authors wish to acknowledge for the assistance extended by Mr. A.P. Muhandiramge, Senior Telecommunications officer (Network Division) and Mr. D.V. Niranjan, Telecommunications officer, of the Telecommunications Regulatory Commission of Sri Lanka upon completion of this research.

References

[1] Elert, G., HYPERLINK "http://hypertextbook.com/physics/electricity/em-spectrum/" "The Electromagnetic Spectrum, the Physics Hyper textbook". *Hypertextbook.com*. Retrieved 2020-10-16.

[2] Granger, C., Hopkins, J., 'Review of potential health effects of exposure to the radiofrequency electromagnetic field from 5G wireless technology', October 15-2019.

[3] Hardell, L., Nilsson, M., Koppel, T., Carlberg, M., Aspects on the International Commission on Nonionizing Radiation Protection (ICNIRP) 2020 Guidelines on Radiofrequency Radiation. Journal of Cancer Science and Clinical Therapeutics 5 (2021): 250-285.

[4] Trifield EMF meter user manual, v1.0.1 March 2018 © 2018 Alpha Lab, Inc. https://manuals.plus/wp-content/uploads/2021/04/910SgBBfL4L.pdf

[5] Narda safety test solutions 'Narda broadband field meter Safety manual,2013/35/EU, www.narda-sts.com

[6] High Performance Handheld Spectrum Analyzer 'User Guide Spectrum Master™ MS2720T'. Copyright 2020 Anritsu Company, 490 Jarvis Drive Morgan Hill, CA 95037-2809 USA. http://www.anritsu.com

[7] Software-defined multirole jammer for vehicle-based patrol activities. https://www.gew.co.za/electronic- warfare/products/gmj9-multirole-jammer/

[8] Shaw, J.A., Radiometry and the Friis transmission equation, Department of Electrical & Computer Engineering, Montana State University, Bozeman, Montana 59717.

[9] Kraus, J. D., (1950). Antennas. McGraw-Hill. Chapter 3, ‘The antenna as an aperture, p. 30.

[10] Xu, Y., Chi, B., Yu, X., Qi, X., Chiang, P., and Wang Z., Power-scalable, complex band pass/low-pass Filter with I/Q imbalance calibration for a multimode GNSS receiver. IEEE Transactions on Circuits & Systems II Express Briefs 59 (2012), 30-34.

[11] Gabbar, H.A., Othman, A.M., Abdussami, M.R., Review of Battery Management Systems (BMS) Development and Industrial Standards. Technologies 2020, 9, 28. https://doi.org/10.3390/ technologies9020028

[12] Lee, S., Kim, J., Power Capability Analysis of Lithium Battery and Super capacitor by Pulse Duration. Electronics 2019, 8, 1395.

[13] Telecommunications Regulatory Commission of Sri Lanka Regulatory Guidelines for the Use of 2.4 GHz and 5GHz Bands to Deploy Outdoor Wireless Local Area Networks (WLAN). https://www.trc.gov.lk/images/pdf/ RegulatoryGuidelinesForOutdorWLAN.pdf

Author Biographies

Lakshitha Rangana WICKRAMASINGHE. received his B.Sc. (Hon) degree from The Open university of Sri Lanka. He is currently working as an Engineering assistant in Sri Lanka Telecom PLC. His main research interests include Communications, IoT based applications and image processing.

Email: Wick520@gmail.com

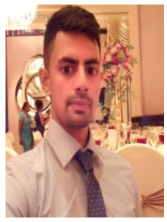

Sisaara PERERA. received his B.Sc. (Hon) degree from The Open university of Sri Lanka. He is currently a Lecturer attached to the Department of Electrical and Computer engineering at the same university. His main research interests include Machine vision, image processing, Robotics, Nano-engineering and applications.

Email: msper@ou.ac.lk

Annexure 1

Table 2 Power densities measured near and far field to the tower in District of Galle

Tower 1	Distance(m)	10	20	30	40	50	60	70	80	90	100	Time average ICNIRP* Threshold power density level	Hazard Level
Power Density (W/m^2)	900MHz	0.00064	0.00065	0.00066	0.00065	0.00065	0.00062	0.00062	0.00062	0.00061	0.00061	4.5	Null
Power Density (W/m^2)	1800MHz	0.00196	0.00198	0.00199	0.00198	0.00199	0.00193	0.00192	0.00191	0.00190	0.00189	2	Null
Power Density (W/m^2)	2400MHz	0.00354	0.00357	0.00357	0.00361	0.00362	0.00328	0.00326	0.00325	0.00323	0.00320	10	Null
Tower 2													
Power Density (W/m^2)	900MHz	0.00058	0.00060	0.00062	0.00064	0.00065	0.00060	0.00061	0.00061	0.00062	0.00062	4.5	Null
Power Density (W/m^2)	1800MHz	0.00200	0.00201	0.00202	0.00202	0.00205	0.00160	0.00162	0.00163	0.00163	0.00163	2	Null
Power Density (W/m^2)	2400MHz	0.00350	0.00352	0.00356	0.00360	0.00365	0.00320	0.00321	0.00320	0.00322	0.00323	10	Null
Tower 3													
Power Density (W/m^2)	900MHz	0.00068	0.00068	0.00069	0.00069	0.00071	0.00055	0.00055	0.00056	0.00058	0.00059	4.5	Null
Power Density (W/m^2)	1800MHz	0.00196	0.00197	0.00195	0.00196	0.00198	0.00172	0.00177	0.00179	0.00178	0.00178	2	Null
Power Density (W/m^2)	2400MHz	0.00370	0.00372	0.00374	0.00375	0.00379	0.00318	0.00319	0.00322	0.00324	0.00325	10	Null

Continued 2

Tower 4	Distance(m)	10	20	30	40	50	60	70	80	90	100	Time average ICNIRP* Threshold power density level	Hazard Level
Power Density (W/m^2)	900MHz	0.00063	0.00063	0.00064	0.00066	0.00067	0.00054	0.00054	0.00055	0.00056	0.00057	4.5	Null
Power Density (W/m^2)	1800MHz	0.00194	0.00194	0.00195	0.00195	0.00196	0.00165	0.00166	0.00165	0.00166	0.00167	2	Null
Power Density (W/m^2)	2400MHz	0.00350	0.00351	0.00351	0.00353	0.00354	0.00318	0.00318	0.00320	0.00320	0.00321	10	Null
Tower 5													
Power Density (W/m^2)	900MHz	0.00060	0.00062	0.00062	0.00063	0.00064	0.00057	0.00058	0.00059	0.00059	0.00063	4.5	Null
Power Density (W/m^2)	1800MHz	0.00197	0.00198	0.00199	0.00200	0.00205	0.00180	0.00183	0.00184	0.00185	0.00186	2	Null
Power Density (W/m^2)	2400MHz	0.00361	0.00362	0.00366	0.00367	0.00369	0.00340	0.00343	0.00347	0.00350	0.00352	10	Null
Tower 6													
Power Density (W/m^2)	900MHz	0.00080	0.00082	0.00083	0.00084	0.00086	0.00078	0.00078	0.00079	0.00080	0.00080	4.5	Null
Power Density (W/m^2)	1800MHz	0.00200	0.00203	0.00205	0.00209	0.00215	0.00193	0.00193	0.00195	0.00196	0.00196	2	Null
Power Density (W/m^2)	2400MHz	0.00375	0.00377	0.00382	0.00384	0.00390	0.00358	0.00358	0.00359	0.00359	0.00360	10	Null

Annexure 2

Table 3 Calibration results of the prototype with the standard Anritsu MS 2720T spectrum analyzer

dBm	Power in (mW)	Power in Watt	Measured DC voltage from 900MHz Rx antenna for Rx power	Power density for 900MHz in W/m2	Measured DC voltage from 1800MHz Rx antenna for Rx power	Power density for 1800MHz in W/m2	Measured DC voltage from 2450MHz Rx antenna for Rx power	Power density for 2450MHz in W/m2
0	1	0.001	1.96	0.049779772	1.97	0.150524147	1.98	0.27870606
–1	0.794328235	0.000794328	1.88	0.039541479	1.96	0.11956558	1.96	0.221384093
–2	0.630957344	0.000630957	1.63	0.031408913	1.96	0.094974316	1.96	0.175851636
–3	0.501187234	0.000501187	1.38	0.024948986	1.38	0.075440781	1.50	0.139683919
–4	0.398107171	0.000398107	1.25	0.019817684	1.25	0.059924742	1.38	0.110954881
–5	0.316227766	0.000316228	1.19	0.015741746	1.25	0.047599915	1.30	0.088134595
–6	0.251188643	0.000251189	1.13	0.012504113	1.13	0.037809956	1.23	0.070007797
–7	0.199526231	0.000199526	1.05	0.00993237	1.03	0.030033516	1.06	0.05560917
–8	0.158489319	0.000158489	1.00	0.007889562	1.00	0.02385647	1.00	0.044171934
–9	0.125892541	0.000125893	0.99	0.006266902	0.90	0.018949867	0.97	0.035087014
–10	0.1	0.0001	0.99	0.004977977	0.85	0.015052415	0.95	0.027870606
–11	0.079432823	7.94328E-05	0.98	0.003954148	0.85	0.011956558	0.97	0.022138409
–12	0.063095734	6.30957E-05	0.98	0.003140891	0.90	0.009497432	0.97	0.017585164
–13	0.050118723	5.01187E-05	1.00	0.002494899	0.95	0.007544078	1.00	0.013968392
–14	0.039810717	3.98107E-05	1.01	0.001981768	0.95	0.005992474	1.00	0.011095488
–15	0.031622777	3.16228E-05	1.03	0.001574175	1.00	0.004759991	0.98	0.008813459
–16	0.025118864	2.51189E-05	1.03	0.001250411	0.95	0.003780996	0.95	0.00700078
–17	0.019952623	1.99526E-05	1.00	0.000993237	1.00	0.003003352	0.99	0.005560917
–18	0.015848932	1.58489E-05	0.99	0.000788956	1.01	0.002385647	1.00	0.004417193
–19	0.012589254	1.25893E-05	0.99	0.00062669	1.00	0.001894987	0.99	0.003508701
–20	0.01	0.00001	0.98	0.000497798	1.00	0.001505241	0.99	0.002787061
–21	0.007943282	7.94328E-06	1.00	0.000395415	1.01	0.001195656	1.00	0.002213841
–22	0.006309573	6.30957E-06	1.01	0.000314089	1.03	0.000949743	1.00	0.001758516

Continued 3

dBm	Power in (mW)	Power in Watt	Measured DC voltage from 900MHz Rx antenna for Rx power	Power density for 900MHz in W/m2	Measured DC voltage from 1800MHz Rx antenna for Rx power	Power density for 1800MHz in W/m2	Measured DC voltage from 2450MHz Rx antenna for Rx power	Power density for 2450MHz in W/m2
−23	0.005011872	5.01187E-06	1.03	0.00024949	1.03	0.000754408	1.06	0.001396839
−24	0.003981072	3.98107E-06	1.02	0.000198177	1.03	0.000599247	1.03	0.001109549
−25	0.003162278	3.16228E-06	1.01	0.000157417	1.03	0.000475999	1.02	0.000881346
−26	0.002511886	2.51189E-06	1.00	0.000125041	1.01	0.0003781	1.01	0.000700078
−27	0.001995262	1.99526E-06	0.99	9.93237E-05	1.00	0.000300335	1.02	0.000556092
−28	0.001584893	1.58489E-06	0.98	7.88956E-05	1.03	0.000238565	1.03	0.000441719
−29	0.001258925	1.25893E-06	0.99	6.2669E-05	0.99	0.000189499	1.01	0.00035087
−30	0.001	0.000001	1.00	4.97798E-05	0.98	0.000150524	1.00	0.000278706
−31	0.000794328	7.94328E-07	0.99	3.95415E-05	0.99	0.000119566	0.99	0.000221384
−32	0.000630957	6.30957E-07	1.00	3.14089E-05	1.00	9.49743E-05	0.99	0.000175852
−33	0.000501187	5.01187E-07	1.00	2.4949E-05	1.00	7.54408E-05	0.99	0.000139684
−34	0.000398107	3.98107E-07	1.00	1.98177E-05	1.00	5.99247E-05	0.96	0.000110955
−35	0.000316228	3.16228E-07	0.97	1.57417E-05	0.99	4.75999E-05	0.95	8.81346E-05
−36	0.000251189	2.51189E-07	0.97	1.25041E-05	0.99	3.781E-05	0.94	7.00078E-05
−37	0.000199526	1.99526E-07	0.97	9.93237E-06	0.99	3.00335E-05	0.99	5.56092E-05
−38	0.000158489	1.58489E-07	1.00	7.88956E-06	0.99	2.38565E-05	0.98	4.41719E-05
−39	0.000125893	1.25893E-07	1.05	6.2669E-06	0.99	1.89499E-05	0.97	3.5087E-05
−40	0.0001	0.0000001	1.06	4.97798E-06	0.99	1.50524E-05	0.98	2.78706E-05
−41	7.94328E-05	7.94328E-08	1.06	3.95415E-06	1.00	1.19566E-05	1.00	2.21384E-05
−42	6.30957E-05	6.30957E-08	1.07	3.14089E-06	1.01	9.49743E-06	1.03	1.75852E-05
−43	5.01187E-05	5.01187E-08	1.08	2.4949E-06	1.05	7.54408E-06	1.08	1.39684E-05
−44	3.98107E-05	3.98107E-08	1.09	1.98177E-06	1.08	5.99247E-06	1.08	1.10955E-05
−45	3.16228E-05	3.16228E-08	1.10	1.57417E-06	1.08	4.75999E-06	1.08	8.81346E-06
−46	2.51189E-05	2.51189E-08	1.11	1.25041E-06	1.08	3.781E-06	1.08	7.00078E-06
−47	1.99526E-05	1.99526E-08	1.12	9.93237E-07	1.06	3.00335E-06	1.11	5.56092E-06
−48	1.58489E-05	1.58489E-08	1.13	7.88956E-07	1.06	2.38565E-06	1.17	4.41719E-06